Atomic Physics Experiments

Rachel Domagalski
Partner: Matthew Turner

November 18, 2013

Abstract

Atomic physics experiments serve as tests which can measure important physical constants. This lab presents two classic atomic physics experiments, in which the Rydberg constant and the Bohr magneton are measured. The experiment that measures the Rydberg constant is done through measuring the Balmer series spectral lines. The Bohr magneton is measured from Zeeman splitting. The value of the Rydberg constant determined from fitting to the Rydberg formula was measured to be $R = 1.095 \times 10^7 \pm 2 \times 10^4\ m^{-1}$. The measured value of the Bohr magneton was found to be $\mu_B = 1.49 \times 10^{-23} \pm 2 \times 10^{-25}\ J/T$.

1 Introduction

Quantum mechanics has incredible importance in understanding the structure of atoms. Therefore, atomic physics experiments serve as good experimental tests to see if quantum mechanics is a valid theory, and studying spectral lines is useful in testing quantum mechanics. Initially, when physicists first started observing the spectrum of various elements, they discovered that the spectra did not consist of continuous bands of color, but of sharp and discrete lines of various colors. Classical physics did not provide any explanation for why this happened. Quantum mechanics, however, was able to predict the wavelengths of the spectral lines, as well as explain atomic interactions that gave rise to these spectral lines.

In quantum mechanics, energy comes in discrete packets, called quanta. This is different from classical mechanics where the energy distributions are continuous. The standard interpretation of quantum mechanics is that a system can be described by a wavefunction Ψ, which is a linear combination of the eigenvectors of the system's Hamiltonian operator. Since the Hamiltonian is a Hermitian operator, it's eigenvalues are observable quantities and the eigenvalues of the Hamiltonian represent the energy of the system. In practice, the energy levels are not directly measured, but the energy level differences can be measured by measuring the wavelengths or frequencies of the light that gets absorbed or emitted when a quantum system changes states. The spectra that arises from the energy level changes can serve as a good probe of the quantum system being measured.

Two areas of interest in atomic physics are the hydrogen and helium atoms. Hydrogen is interesting because it is the only atom for which the Schrödinger equation can be solved analytically for the energy levels. It should be noted that in the case of hydrogen, solving the Schrödinger equation is not the only method to calculate the hydrogen energy levels. The other method, which only works for hydrogen, is the Bohr model, but this model is very limited. The energy levels of hydrogen will be measured in the lab and will be used to calculate the Rydberg constant.

Helium is an interesting atom to study because it provides a simple two-level system and experiments with Helium can be used to test perturbation theory. One example of a system that requires perturbation theory to predict experimental results is known as Zeeman splitting. Zeeman splitting is the effect which occurs when electrons are placed in an external magnetic field. The reason that it is called splitting is because energy levels which were degenerate without the external field split and become non-degenerate when the field is applied. When observed in the lab, this corresponds to a splitting of the spectral lines of an atom. This effect can be used to measure the Bohr magneton.

2 The Balmer Series

The hydrogen atom can be approximated as point charge e^- of mass m in a Coulomb potential from a positive charge e. The Schrödinger equation for that system is [1]

$$\left[-\frac{\hbar^2}{2m}\nabla^2 - \frac{e^2}{4\pi\epsilon_0 r}\right]\psi = E\psi \tag{1}$$

The eigenvalues for (1) are [1]

$$E_n = -\frac{m}{2\hbar^2}\left(\frac{e^2}{4\pi\epsilon_0}\right)^2 \frac{1}{n^2} \approx -\frac{13.6\ eV}{n^2} \tag{2}$$

When electrons transition from energy levels, they emit photons with energy $E = hc/\lambda$, which is equal to the difference between the energy levels of the transition. Many different energy level transitions have been given names, and the Balmer series is defined as transitions down to the $n = 2$ energy level. From this, it is easy to derive the Rydberg formula that gives the Balmer lines.

$$\frac{1}{\lambda_n} = R\left(\frac{1}{4} - \frac{1}{n^2}\right), \text{ where } R = \frac{m_e e^4}{8\epsilon_0^2 h^3 c} \tag{3}$$

The Balmer series is special because it is the only class of energy level transitions for hydrogen that produces emission lines in the visible spectrum. The experiment involving hydrogen seeks to measure the Rydberg constant from measuring the Balmer wavelengths. It can be seen from (3) that the Rydberg constant can be measured in two places, the slope and the intercept, from creating a linear fit of $1/n^2$ and $1/\lambda$.

2.1 Experimental setup

This experiment uses a spectrometer connected to a photomultiplier tube to measure the emission lines of hydrogen (see Figure 1). How this works is that light from a hydrogen lamp gets focused into a spectrometer. Inside the spectrometer are two mirrors and a diffraction grating, which are used to reflect the light. The diffraction grating also has the function of splitting the light which helps get better resolution on the wavelengths of light. The light then moves on to the photomultiplier tube, which converts the light into an electrical signal so it can be recorded. The data acquisition process of the experiment is done with a digital multimeter that has a GPIB output that gets fed into a computer running LabVIEW.

The experimental setup is pretty simple and straightforward. However, there are some uncertainties in the measurements that must be accounted for. The first uncertainty is the wavelength resolution of the spectrometer. The spectrometer has a resolving power, which is defined as [2]

$$R \equiv \frac{\lambda}{\Delta\lambda} \tag{4}$$

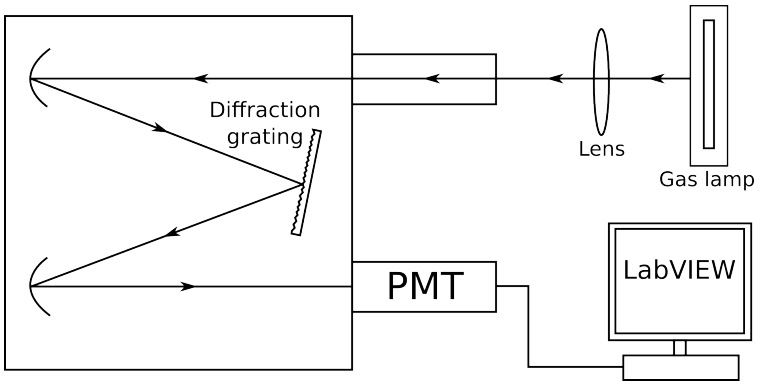

Figure 1: Block diagram of the spectrometer used to measure the Balmer lines.

In the case of diffraction gratings, the resolving power is [2]

$$\frac{\lambda}{\Delta\lambda} = mN \tag{5}$$

where N is the number of grooves in the diffraction grating and m is an integer related to the propagation modes of the diffraction. For this experiment, $m = 1$, and since the diffraction grating in the lab has 300 grooves per millimeter [3] and since the slit width of the spectrometer can be adjusted from 0.005 mm to 3 mm, the resolving power of the grating is about 300.

2.2 Line Broadening

The second uncertainty in the wavelength comes from spectral line broadening. While (3) predicts sharp peaks in the spectrum at certain wavelengths, very sharp distributions with nonzero widths are measured around the absorption or emission peaks. This width in wavelength or frequency is what is known as spectral line broadening. Spectral broadening has several causes, three of which will be discussed, and the study of spectral line broadening has useful applications in astrophysics.

The first mechanism of line broadening is called natural broadening. This broadening comes from the Heisenberg uncertainty principle. The Heisenberg uncertainty principle for time and energy states that

$$\Delta E \Delta t \geq \frac{\hbar}{2} \tag{6}$$

For a gas, the line profile that corresponds to natural broadening is [4]

$$\phi_\nu = \frac{\frac{\Gamma}{4\pi^2}}{\Delta\nu^2 + \left(\frac{\Gamma}{4\pi}\right)^2} \tag{7}$$

where $\Delta\nu = \nu - \nu_0$, and Γ is the radiative damping coefficient, which is just the reciprocal of the mean lifetime of a quantum state, which is Δt from the uncertainty principle. The mean lifetime is on the order of 10 ns. The FWHM of (7), which corresponds to $2\Delta\nu$ is equal to $\frac{\Gamma}{2\pi}$ [4], which gives the broadening in frequency space of

$$\Delta\nu = \frac{\Gamma}{4\pi} = \frac{1}{4\pi\Delta t} \tag{8}$$

Since the experiment measures wavelengths and not frequencies, line broadening values in frequency space will have to be converted to wavelength space. The equation relating the frequency and wavelength of light waves $\lambda\nu = c$, can be differentiated to get a relation for small spectral differences. This gives $\nu d\lambda = -\lambda d\nu$ or $\nu\delta\lambda = \lambda\delta\nu$, where the signs of the differences are neglected since line broadening occurs in both directions with respect to a peak spectral line. From this, a relation between small wavelength shifts and small frequency shifts can be found to be

$$\delta\lambda = \frac{\lambda^2}{c}\delta\nu \tag{9}$$

The above relation can be used to get the natural line broadening width in wavelength space. Plugging (8) into (9) gives

$$\Delta\lambda \approx \frac{\lambda^2}{4\pi c\Delta t} \tag{10}$$

The relation for line broadening in wavelength space that was derived from the Lorentz profile (7) can also be derived directly from the uncertainty principle, since $\Delta E = h\Delta\nu = hc\Delta\lambda/\lambda^2$, which can be shown with (9). Plugging this into the uncertainty relation gives

$$\Delta E\Delta t = \frac{hc}{\lambda^2}\Delta\lambda\Delta t \geq \frac{h}{4\pi} \tag{11}$$

Rearranging that gives

$$\Delta\lambda = \frac{\lambda^2}{4\pi c\Delta t} \tag{12}$$

which is the same expression derived from analyzing the Lorentz profile. Plugging in the mean lifetime of 10 ns gives a line broadening of $\Delta\lambda \approx 6 \times 10^{-5}$ Åfor wavelengths of 500 nm. Clearly, natural broadening does not play a huge role as a line broadening mechanism. There is a second type of line broadening called pressure broadening, which is caused by collisions between particles. This causes the lifetime of each state to decrease, which will increase the radiative damping factor, which will increase line broadening. However, the size of this broadening is clearly on the same order of natural broadening.

Another type of line broadening comes from thermal Doppler broadening. The cause of this broadening comes from the motion of atoms in a gas moving fast so that they have some Doppler shift. The broadening profile for thermal Doppler profile can be found using the Maxwell-Boltzman distribution for the velocities of particles parallel to the line of sight of an observer, which is [4]

$$f\left(v_{\parallel}\right)dv_{\parallel} = \sqrt{\frac{m}{2\pi kT}}e^{\frac{mv_{\parallel}^2}{2kT}}dv_{\parallel} \tag{13}$$

One can use the above distribution, plus the relations $f\left(v_{\parallel}\right)dv_{\parallel} = f\left(\nu\right)d\nu$ and $\nu = \nu_0\left(1 + v_{\parallel}/c\right)$ to get a frequency profile proportional to

$$e^{-\frac{mc^2}{2kT}\frac{\Delta\nu^2}{\nu_0^2}} \tag{14}$$

where $\Delta\nu = \nu - \nu_0$. The HWHM frequency difference for this distribution is

$$\Delta\nu = \nu_0\sqrt{\frac{2kT\ln\left(2\right)}{mc^2}} \tag{15}$$

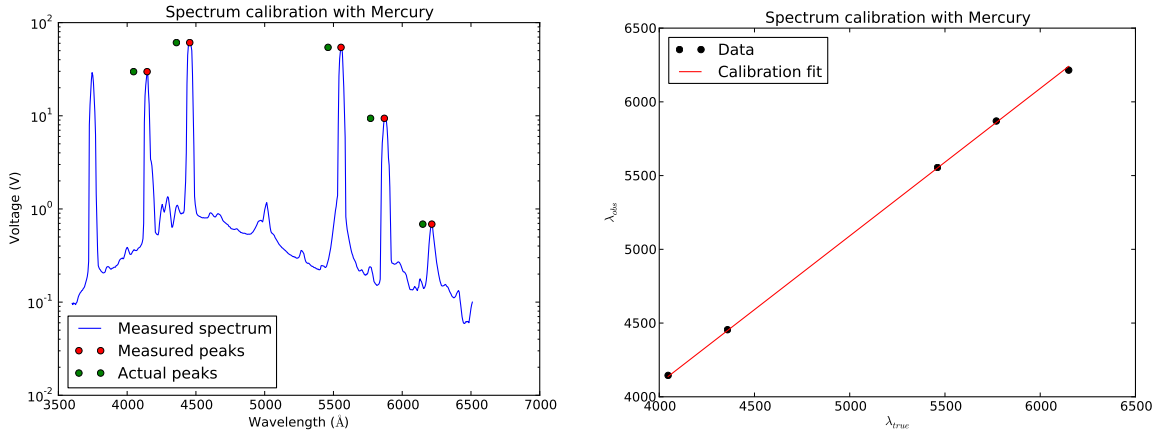

Figure 2: (left) Spectrum of mercury, plus a comparison of the observed peaks vs the average peaks illustrating the calibration that needed to be made. (right) Calibration plot relating the observed spectral lines of mercury to the accepted line values.

and this corresponds to a frequency spaced line broadening of

$$\Delta\lambda = \lambda_0 \sqrt{\frac{2kT\ln(2)}{mc^2}} \tag{16}$$

If it is assumed that the temperature inside of the gas is approximately 600 K, then the line width due to thermal Doppler broadening is approximately 4×10^{-2} Å, which is much larger than natural broadening but is still small.

2.3 Calibration

Data collection is done by scanning through a range of wavelengths on the spectrometer and recording the signal corresponding to each wavelength in LabVIEW. This is pretty straightforward, but there are corrections that need to be made to the wavelengths that the spectrometer claims versus actual wavelength values. The calibration curve for this is done by measuring the spectrum of mercury and correcting it using the accepted values of the emission lines for mercury. Mercury's spectrum, plus the calibration curve used to correct the wavelengths, can be seen in Figure 2. The calibration curve is fairly straightforward to add to the measured wavelengths and should give the correct wavelengths.

2.4 Analysis

Calculating the Rydberg constant from (3) is fairly straightforward. This is done first by correcting the measured wavelengths that LabVIEW records using the calibration curve generated from the spectrum of mercury. Next, the peaks in the spectrum are detected and mapped to the quantum number that corresponds to the emission line. This can be done by noting that the distances in wavelengths in Figure 3 seem to get smaller, maybe as $1/n^2$, when moving from left to right. It can be seen from (3) and Figure 3 that the inverse wavelength is linearly proportional to $1/n^2$. The fit can then be used to to calculate Rydberg's constant from both the slope ($m = -R$) and the y-intercept ($b = R/4$). The weighted average of the two measurements of R can be taken to calculate a final value of R.

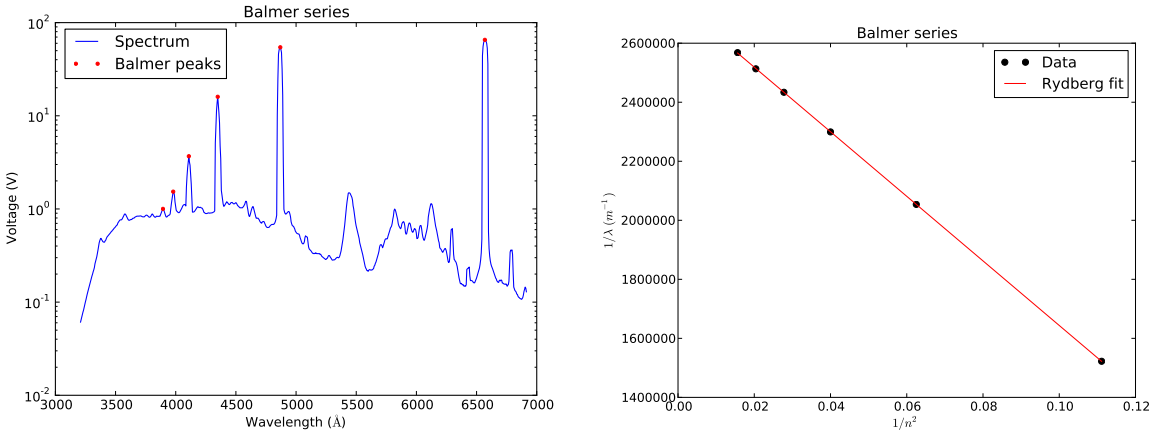

Figure 3: (left) The spectrum of hydrogen for visible wavelengths. Note that the wavelengths peaks get closer and closer together when moving from left to right, like $1/n^2$. (right) Linear fit between $1/\lambda$ and $1/n^2$.

In order to compute the weighted average for any measurement of a specific value, one must know the uncertainties on each term being used to compute the average. This can be done by using the definition of χ^2, and the condition that the best fit yields a $\chi^2/ndf = 1$. Assuming that the error for all inverse wavelength is constant, it can easily be shown that

$$\sigma^2 = \frac{1}{ndf}\sum_{i=0}^{N}(y_i - mx_i - b)^2 \tag{17}$$

This can be used to give the errors of the coefficients computed in the linear fit which are [5]

$$\begin{aligned} \sigma^2(m) &= \left(\frac{1}{\sigma^2}\sum x_i^2\right)^{-1} \\ \sigma^2(b) &= \frac{\sigma^2}{N} + \langle x\rangle^2\sigma^2(m) \end{aligned} \tag{18}$$

where $\langle x\rangle = \langle 1/n^2\rangle$ and N is the number of data points used in the least squares fit. Applying this to the two values of R gives a value of $R = 1.095 \times 10^7 \pm 2 \times 10^4\ m^{-1}$. This is pretty close to the accepted value of the Rydberg constant, although it seems as the error is way too small.

3 Zeeman Splitting

Zeeman splitting is the effect that occurs when electrons are placed in an external magnetic field. What happens is that when the magnetic field is applied to the electrons, the energy levels, which are degenerate, split and become either non-degenerate or less degenerate. This experiment uses helium gas to measure the Zeeman splitting, and the Hamiltonian for the electrons is

$$\hat{H} = -\vec{\mu}\cdot\vec{B}_{ext} \tag{19}$$

where $\vec{\mu}$ is the magnetic moment of the electron. Quantum mechanics shows that the energy separation of the splitting is [1]

$$\Delta E = m_J g_J \mu_B B_{ext} \tag{20}$$

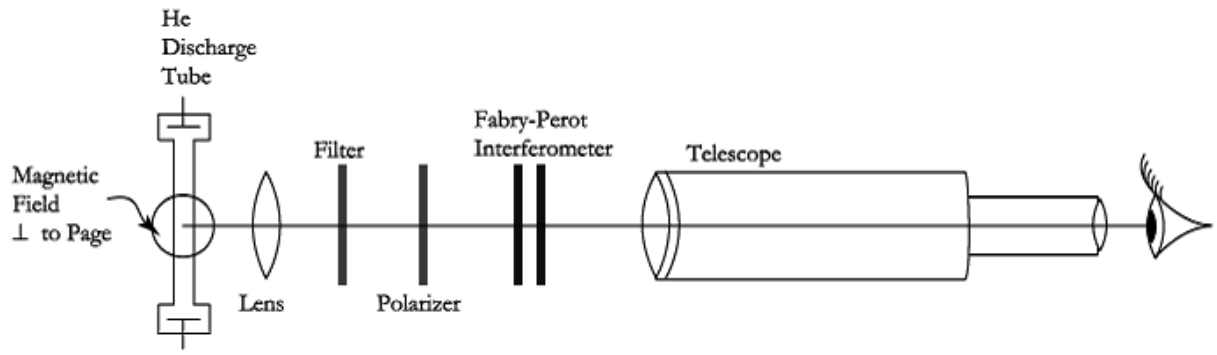

Figure 4: Block diagram of the Zeeman splitting experiment.

where m_J is the quantum number describing the total momentum in the $\hat{z}$ direction, g_J is the famous Lande-g factor, and μ_B is the Bohr magneton. The actual effect of Zeeman splitting is very small and it takes a precision measurement in order to observe it. In this experiment, Zeeman splitting of the red spectral line of helium was measured, and that corresponds to a state change of ${}^1D \rightarrow {}^1P$.

3.1 Experimental Setup

A block diagram of the Zeeman splitting experiment can be seen in Figure 4. This experiment measures the Zeeman splitting by observing ring shapes in an image. How it works is that a helium discharge tube is placed inside of a pair of Helmholtz coils. Light emitted from the gas tube gets focused through a red filter, which removes most of the spectral lines. After the light goes through the filter, it passes through a polarizer, which is set to only admit frequencies coming from energy level splittings of $\Delta m_J = \pm 1$. The polarized light then passes through a Fabry-Perot interferometer, which is used because it has a high wavelength resolving power. After the light goes through the interferometer, it gets recorded by a CCD camera and in the rare case that the camera software (or even Windows) on the computer the camera is connected to is actually working properly, or at all, a bitmap of the Zeeman rings can be taken and saved.

3.2 The Fabry-Perot Interferometer

The Fabry-Perot interferometer is what allows the Zeeman splitting to be observed. A diagram demonstrating the basics of how it works can be seen in Figure 5. The interferometer is made of two partially reflecting mirrors and a lens. How the interferometer works is that an incoming beam of light enters the interferometer, and then gets reflected off on the second mirror. Part of the light beam goes through the mirror and another part gets reflected back to the first mirror, which then reflects another ray of light at the second mirror at the same angle of incidence as the original beam. All of the beams that were generated from the original beam and the mirror sequence then pass through the lens in the interferometer, which is designed to focus the beams at infinity. The beams that come out of the lens produce and intensity distribution of [3]

$$I(\theta, t) = \frac{I_0}{1 + \dfrac{4R}{(1-R)^2} \sin^2 \dfrac{\delta}{2}} \tag{21}$$

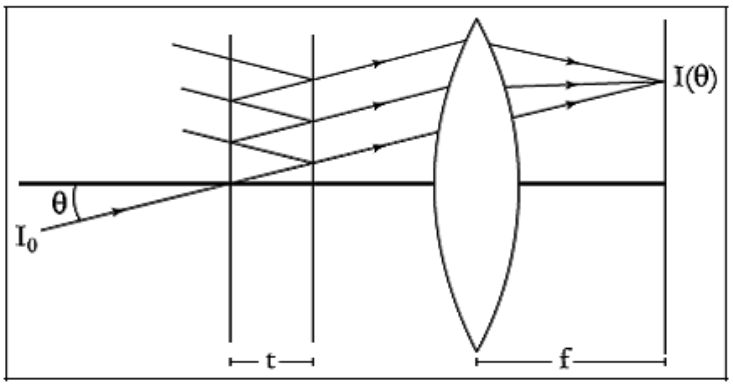

Figure 5: Schematic diagram of the workings of the Fabry-Perot interferometer.

where $\delta = 2\pi\frac{2t\cos\theta}{\lambda}$, t is the spacing of the interferometer, and R is the reflectance of the mirrors in the interferometer. The smallest difference in wavenumber that can be resolved, which corresponds to the smallest energy difference that can be resolved, is [3]

$$\delta\sigma = \frac{1}{2tN_R} \tag{22}$$

and

$$N_R = \pi\frac{\sqrt{R}}{1-R} \tag{23}$$

For the interferometer used in the experiment, t is 8.1 mm and R is 0.90, so $N_R = 29.8$ and $\delta\sigma = 2.07\ m^{-1}$.

3.3 Zeeman Rings

An example of data from this experiment can be seen in Figure 6. In that case, there is no magnetic field being applied to the helium gas. When a magnetic field does get applied to the helium, the rings start to split. There are two splittings of interest in this experiment, which can be seen in Figure 7. The exact procedure for using these images to calculate the Bohr magneton shall be described in the next section. However, it should be noted that originally, a calibration curve to map the voltage applied to the Helmholtz coils to the magnetic field produced by the coils was made. However, since there were only two Zeeman splittings of interest for the final analysis, directly measuring the magnetic field for those two splittings seemed to be simpler.

3.4 The Bohr Magneton

The Zeeman splitting experiment can be used to get a measurement of the Bohr magneton μ_B. The energy difference between the split levels is $\Delta E = hc\Delta\nu$. In this experiment, the value of $\Delta\nu$ is known to be [6]

$$\Delta\nu = \frac{\Delta n}{2t} \tag{24}$$

where Δn is the fractional difference in the splitting of the Zeeman rings and t is the spacing of the Fabry-Perot interferometer. Setting the energy difference equal to the splitting energy difference gives

$$\frac{hc\Delta n}{2t} = \mu_B B_{ext} \tag{25}$$

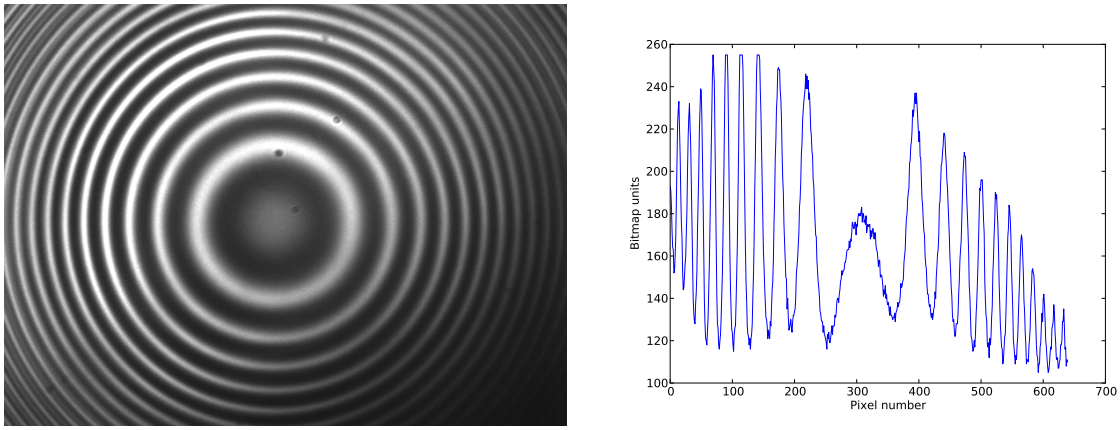

Figure 6: (left) Bitmap of the Zeeman rings. (right) The center row of the left image. No magnetic field is currently being applied to the helium.

where m_J and g_J are both equal to one. This gives an expression for the Bohr magneton that relates to the quantities measurable in the experiment as

$$\mu_B = \frac{hc\Delta n}{2tB_{ext}} \tag{26}$$

The main uncertainty that comes into (26) is from uncertainty in the magnetic field, and this is assuming that any uncertainty in the Fabry-Perot thickness is negligible. Since the variance of the Bohr magneton and the external magnetic field are related as $\sigma_\mu^2/\mu^2 = \sigma_B^2/B^2$, it can easily be demonstrated that

$$\sigma_{\mu_B} = \frac{hc\Delta n}{2tB_{ext}^2}\sigma_B \tag{27}$$

Figure 7 shows the two Zeeman splittings of interest. The magnetic fields measured for these fields were $B_{ext} = 0.278\ T$ when $\Delta n = 1/3$ and $B_{ext} = 0.410\ T$ when $\Delta n = 1/2$. In both cases, the uncertainty of the field is about $0.005\ T$. These values of the magnetic fields give measurements of the Bohr magneton of $\mu_B = 1.47 \times 10^{-23}\ J/T$ and $\mu_B = 1.50 \times 10^{-23}\ J/T$. These values, along with their uncertainties, give a weighted average of $\mu_B = 1.49 \times 10^{-23} \pm 2 \times 10^{-25}\ J/T$. This is on the right order of magnitude of the Bohr magneton, but both measured values are off by a scaling factor, which seems constant. The magnetic field detector used in the experiment was checked against a source of known value and seemed to be working properly. It's possible that there could be an error in the value given for t, but the range of t is small, so that wouldn't explain everything.

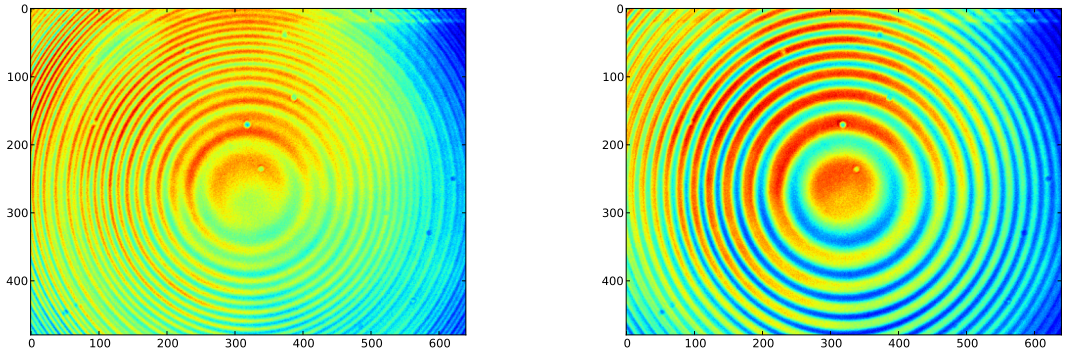

Figure 7: (left) Evenly spaced rings from the splitting corresponds to a $\Delta n = 1/3$. (right) Overlapping rings from the splitting corresponds to $\Delta n = 1/2$. Both images have been colorized to make the splitting more clear looking.

References

[1] B.H. Bransden and C.J. Joachim. *Quantum Mechanics*. Pearson Prentice Hall, Second edition, 2000.

[2] E. Hecht and A. Zahac. *Optics*. Addison-Wesley Pub Co., 1974.

[3] D. Orlando. Atomic Physics, 2013. http://labs.physics.berkeley.edu/mediawiki/index.php/Atomic_Physics.

[4] F. LeBlanc. *An Introduction to Stellar Astrophysics*. Wiley, Second edition, 2011.

[5] L. Lyons. *A Practical Guide to Data Analysis for Physical Science Students*. 1991.

[6] A.C. Melissinos. *Experiments in Modern Physics*. 1996.

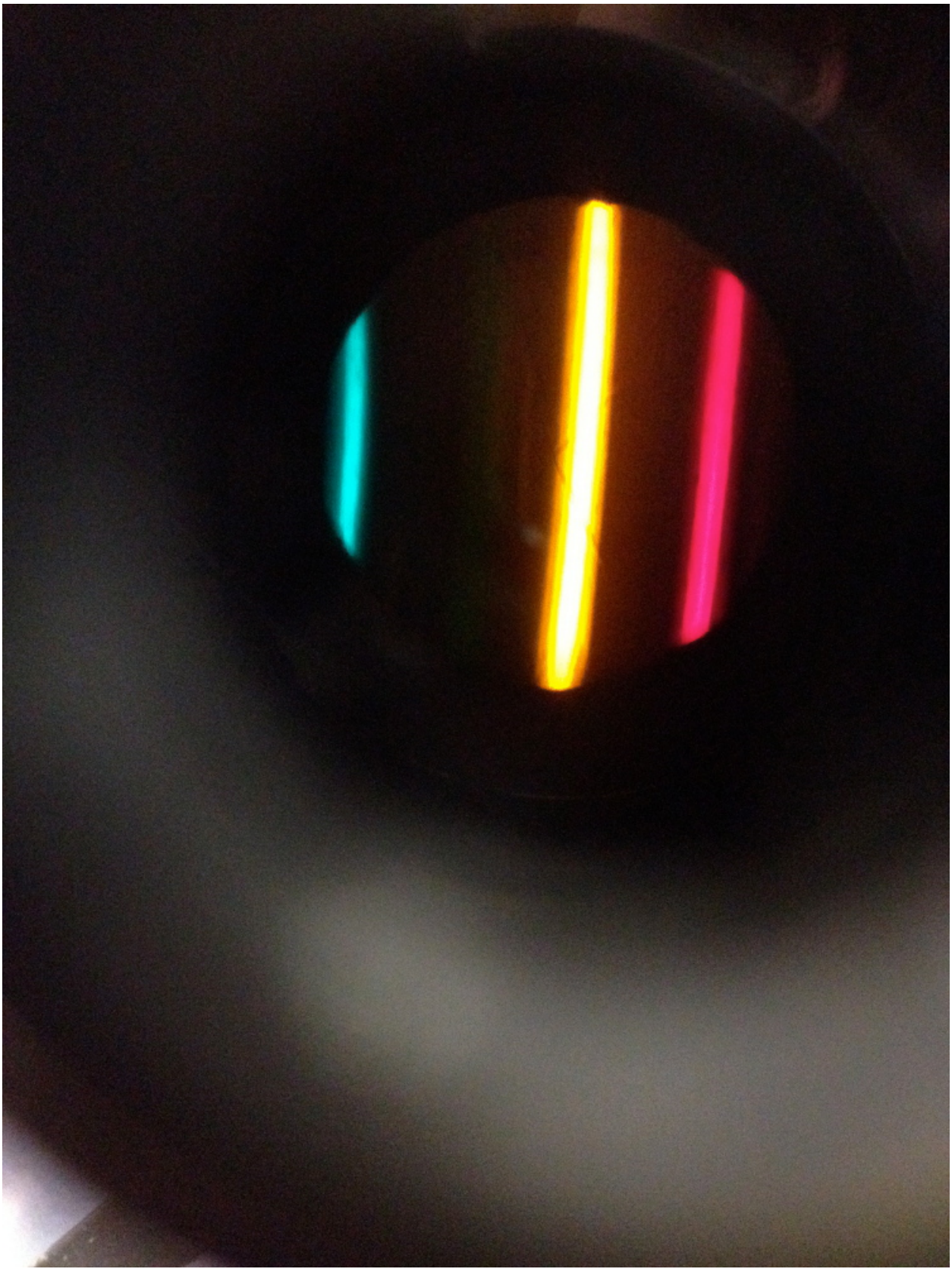

Figure 8: Some of the spectral lines of helium viewed from the prism monochromator.